2

Global histone H3 lysine 27 triple methylation levels are reduced in vessels with advanced atherosclerotic plaques

Rutger J. Wierda, Inge M. Rietveld, Marja C.J.A. van Eggermond, Jeroen A.M. Belien, Erik W. van Zwet, Jan H.N. Lindeman and Peter J. van den Elsen

Life Sciences (2015); **129**, 3–9

Abstract

Aims:

Alterations in epigenetic processes are frequently noted in human disease. These epigenetic processes involve methylation of DNA and post-translational modifications of histones. It is well established that in particular histone methylation plays a key role in gene transcription. In this study, we have investigated the relationship between triple methylation of lysine 27 in histone H3 (H3K27Me3) modifications and atherosclerotic plaque stage.

Materials and Methods:

28 peri-renal aortic tissue patches covering the entire spectrum of atherosclerotic plaque development were evaluated by immunohistochemistry for the levels of H3K27Me3, EZH2, JMJD3 and BMI1.

Key Findings:

The results of our studies are in support of a reduction in global levels of the H3K27Me3 modification in vessels with advanced atherosclerotic plaques. This reduction in H3K27Me3 levels is not accompanied by alterations in global levels of the corresponding histone methyltransferase EZH2, the catalytic subunit of the polycomb repressive complex 2 (PRC2). Likewise no alterations in global levels of BMI1, a component of the PRC1 complex, which binds to H3K27Me3-modified histones or the global expression levels of the histone demethylase JMJD3, which removes the methyl marks on H3K27, were observed.

Significance:

Together, our data show that in atherosclerosis development alterations in global levels of H3K27Me3 occur. The reduction in the number of nuclei in the *tunica media* that display the repressive H3K27Me3 mark in vessels with advanced atherosclerosis plaques therefore could be a reflection of the dynamic pattern of smooth muscle cell differentiation and proliferation associated with atherosclerotic disease.

Introduction

Risk factors for atherosclerosis include many environmental factors.[1] Not surprisingly, research over the past few years has focused on epigenetic contributions to the disease. Nowadays, we are fully aware of the important involvement of epigenetic processes in the regulation of gene expression (see Geissmann *et al.*[2] and references therein). Understanding these epigenetic processes is critical for our understanding of inflammatory responses and disease.

Epigenetic mechanisms change the accessibility of chromatin.[3] The effect of these epigenetic processes on transcription depends on the presence of various post-translational histone modifications, commonly referred to as the histone code. Epigenetic gene regulation is a dynamic process, although the post-translational modifications themselves are chemically stable. Proteins that put the histone code in effect can be divided into three classes: 'writers', 'erasers', or 'readers'. One of the well-studied post-translational histone modifications is triple methylation of lysine 27 in histone H3 (H3K27Me3), which is linked with transcriptional repression.[4] Loss of H3K27Me3 is associated with cell proliferation (see Moore *et al.*[4] and references therein). Gene silencing via H3K27Me3 is orchestrated by two protein-complexes: the polycomb repressive complex 2 (PRC2), the silencing initiation complex, and the polycomb repressive complex 1 (PRC1); the maintenance complex.[4]

The PRC2 core consists of a number of proteins with enhancer of zeste homolog 2 (EZH2) as the catalytic subunit.[5] As such, EZH2 has been associated with X-inactivation, germline development, stem cell pluripotency, cancer metastasis and cell proliferation.[6,7] The PRC1 complex consists of (amongst others) chromobox homolog (CBX) 2, 4, 6, 7, 8 and B lymphoma Mo-MLV insertion region 1 homolog (BMI1; see Mestas *et al.*[5] and Jonasson *et al.*[8] and references therein). This complex recognizes the H3K27 trimethylation mark via the chromodomain of the CBX proteins, but does not possess methyltransferase activity itself.[8] Although the exact function of BMI1 is still unknown, it has been suggested that H2A ubiquitylation regulates BMI1-mediated gene silencing.[8] Furthermore, reduced expression of BMI1 is associated with cellular senescence.[9]

The histone demethylase jumonji domain containing 3 (JMJD3) removes methylation marks from H3K27.[10] JMJD3 has previously been found to be upregulated under nuclear factor kappa-light-chain-enhancer of activated B cells (NF-κB) mediated inflammatory conditions, providing a link between epigenetic regulation and

inflammation.[11] Furthermore JMJD3 has been found to be upregulated in macrophages after lipopolysaccharide (LPS) exposure.[11,12] In general polycomb group (PcG) proteins are broadly expressed; their expression however, can be modulated by environmental stimuli, thus linking extracellular cues to reprogramming of the epigenome.[13,14]

By using immunohistochemistry (IHC), a recent study in ApoE knockout mouse identified histone lysine methylation marks as contributing factors to atherosclerosis development.[15] In particular, these studies revealed a significant decrease in vSMCs for global H3K27Me3 levels in ApoE+/– mice from ApoE-deficient mothers when fed with a high cholesterol diet. The effect of post-natal high cholesterol diet on global H3K27Me3 levels was also noted when offspring from wild-type mothers and ApoE-deficient mothers were compared.[15]

At the moment, not much is known on the role of epigenetic mechanisms to the pathology of atherosclerosis in humans. In the current study, we therefore have evaluated global H3K27Me3 levels in vessels representing different stages of atherosclerotic plaque development. Furthermore, we also investigated global levels of the writer, eraser and reader of this repressive histone mark in these atherosclerotic vessels. Using IHC with antibodies directed against H3K27Me3, EZH2, BMI1 and JMJD3, and an automated evaluation method we found that the numbers of nuclei that display the H3K27Me3 mark in vessels with more advanced atherosclerotic plaques were reduced. The global decrease in the number of H3K27Me3 immunopositive nuclei in the *tunica media* reveals the different epigenetic states of these cells during progression of atherosclerotic disease.

Materials and Methods

Donor and Tissue sampling

A total of 28 peri-renal aortic tissue patches were studied. The patches were obtained during clinical organ transplantation, as has been described previously.[16] The formalin fixed, paraffin embedded sections where cut in 4 µm thick consecutive slides. Donor age ranged from 12 to 71 years (Table 2–1). Sample collection and handling was performed in accordance with the guidelines of the Medical and Ethical Committee in Leiden, the Netherlands and the code of conduct of the Dutch Federation of Biomedical Scientific Societies (http://www.federa.org/code-goed-gebruik-van-lichaamsmateriaal-2011).

Table 2–1: Classification of aortic tissue according to the classification of the AHA proposed by Stary *et al.*[17]

Stage	Median age	*n*	
		male	female
0 (normal vessel)	42	1	2
1	14	1	2
2	50	3	2
3	55	3	1
4	48	1	2
5	57.5	2	2
6	58	5	1

Immunohistochemistry

Slides were deparaffinised in xylene (Merck, Darmstadt, Germany) and rehydrated in graded ethanol (Merck) into water. Antigen retrieval was performed in 0.01M citric acid (Sigma Aldrich, Zwijndrecht, the Netherlands) buffer, pH 6.0 at 98°C. Slides were stained with the following antibodies against: H3K27Me3 and H3K9Me3 (both repressive histone marks), H3Ac and H3K4Me3 (both active histone marks), EZH2, JMJD3, BMI1, or isotype control (Table 2–2). Depending on the antibody, slides were permeabilized, pre-blocked by human serum (HS) incubation, and/or avidin/biotin-block (Vector Laboratories, Burlingame, CA, USA; Table 2–2). Permeabilization was performed by 5 min. incubation in 0.5% (v/v) Triton® X-100 (Sigma Aldrich) in phosphate buffered saline (PBS), followed by 10 min. incubation in 0.1M glycine in PBS. Pre-blocking with HS (LUMC Pharmacy, Leiden, The Netherlands) was performed by incubating slides for 1h in 5% HS (v/v) in PBS with 0.05% (v/v) Tween® 20 (Sigma Aldrich; PBS-T). Avidin/biotin block (AB block) was performed according to manufacturer's instructions. Primary antibody incubations were all performed overnight in 1% (w/v) bovine serum albumin (Sigma Aldrich) in PBS-T unless noted otherwise. Either goat anti-rabbit (Vector Laboratories) or horse anti-mouse (Vector Laboratories) biotin conjugate was used as secondary antibody, depending on the species (Table 2–2). The secondary antibodies where diluted in PBS-T with goat or horse normal serum (Vector Laboratories; dilution 1:66). Secondary antibody incubation (1h) was followed by incubation with Vectastain ABC (Vector Laboratories). Visualization was performed using 3–3′ -diaminobenzidine tetrachloride (DAB; Sigma Aldrich) and Mayer's haematoxylin (Sigma Aldrich) was used for counterstaining.

Image Analysis

Complete slides where digitized with a digital (microscopic) Mirax slide Scanner system (3DHISTECH, Budapest, Hungary) equipped with a 20× objective with a numerical aperture of 0.75 and a Sony DFW-X710 Fire Wire 1/3″ type progressive SCAN IT CCD (pixel size 4.65 × 4.65 µm). After scanning the locations of the *tunica intima*, *tunica media* and *tunica adventitia* were annotated by hand using the Panoramic Viewer software (3DHISTECH) and exported in the TIFF image-format. The total number of nuclei and the number of positive cells for each slide where counted in an automated fashion using ImageJ (available at http://rsbweb.nih.gov/ij/). Briefly, the algorithm is as follows: slides where separated into haematoxylin and DAB components using the colour deconvolution plugin of Ruifrok and Johnston.[18] The MultiThresholder, with parameter settings "Triangle apply", was used to threshold both the DAB and the haematoxylin specific images. Potential nuclei where identified using particle analysis and subsequently mapped to the haematoxylin counterpart. Nuclei consisting of both DAB and haematoxylin components where considered as positively stained nuclei, thus eliminating possible background staining. The total number of nuclei was counted using particle analysis on the haematoxylin image.

Statistical analysis

The relative numbers of positively stained cells are represented as average ±SEM. The data were analysed using a linear model (ANOVA) with a sex effect, age effect, layer effect, AHA (American Heart Association) score effect and interaction effects. The analysis was performed in R (R, http://www.rproject.org). All tests were performed using t– or F-tests as appropriate. To correct each test for multiple testing a Bonferroni correction was used. Differences were considered to be significant if $p < 0.05$ after multiple testing correction. Correlations were tested using Pearson's correlation based on the total percentage of positive stained nuclei per slide and no discrimination was made between tunica media, tunica adventitia or tunica intima. Pearson's correlation was assessed using the SPSS (IBM) software version 20.0.0.2.

Table 2–2: Antibodies (with respective isotypes), dilutions and blocking steps used for immunohistochemistry.

Antibody reactivity	Manufacturer	Species	Isotype	Catalogue no.	Dilution	Triton permeabilization	Serum Block	AB Block
H3K27Me3	Abcam	mouse	IgG3	ab6002	1:200	no	no	no
H3K4Me3	Abcam	rabbit	IgG (polyclonal)	ab8580	1:30,000	no	no	no
H3K9Me3	Millipore	rabbit	IgG (polyclonal)	07-442	1:750	no	no	no
H3Ac	Millipore	rabbit	IgG (polyclonal)	06-599	1:3,000	no	no	no
EZH2	BD Bioscience	mouse	IgG1	612667	1:400*	yes	no	no
BMI1	Abcam	mouse	IgG1	ab14389	1:400	yes	no	no
JMJD3	Abcam	rabbit	IgG (polyclonal)	ab38113	1:700	no	yes	yes
Isotype control	Santa Cruz	rabbit	IgG (polyclonal)	sc2027	Similar to respective specific antibody			
	DAKO	mouse	IgG1	X0931				
	Abcam	mouse	IgG3	ab18394				

*Diluted in PBS + 1/66 Human serum.

Results

Distribution of H3K27Me3, EZH2, BMI1 and JMJD3 in the vessel wall

H3K27Me3, EZH2, BMI1 and JMJD3 staining was performed on serial cross-sections of 28 different aortic samples. The tissue samples were collected during clinical organ transplantation as has been described previously.[16] Donors varied in age from 12 to 71 years old and samples were specially chosen to cover all stadia (including 3 normal, stage 0, vessels) described by Stary *et al.* (Table 2–1).[17] Representative staining patterns of normal vessels (stage 0) and vessels with advanced atherosclerotic plaques (stage 6) are shown in figure 2–1. It can also be established that the staining appears not homogeneous across the entire section (Figure 2–2). Especially in the *tunica media*, positive staining cells are focally observed (Figure 2–2). Interestingly, this patchy staining does not show any correlation to plaque size or location of the plaque. The presence of these clusters of positive cells most likely reflects different chromatin states within the vessel wall.

The number of stained nuclei was determined following digitization of the slides. The *tunica intima*, *tunica media* and *tunica adventitia* were exported as separate images and by using the ImageJ software package the percentage of positive stained cells was subsequently counted, using an algorithm that only takes nuclear staining into account. The results of these analyses show that, when compared with the levels of intimal staining, the abundance of BMI1, EZH2, H3K27Me3, JMJD3 is significantly more in the adventitia (Figure 2–3). These varying staining patterns might be a reflection of the different cellular compositions of the various vessel wall components.

Relationship between H3K27Me3 levels and plaque stage

To investigate the relationship of global H3K27Me3 abundance and plaque stage, we correlated the percentage of positively stained cells in the complete vessel wall to plaque stage. For this purpose we used the lesion stage classification according to the AHA as proposed by Stary *et al.*[17] The results of these analyses revealed a significant decrease in the number of nuclei that stained positive for the H3K27Me3 mark in vessels with more advanced lesions (Figure 2–4). Interestingly, in these vessels with more advanced lesions there is also a reduction in the number of nuclei that stained positively for BMI1 and JMJD3, albeit that this reduction did not reach statistical significance (Figure 2–4). The EZH2 levels showed no significant difference between vessels with early and late stage plaques (Figure 2–4).

Since sex is considered a risk factor for atherosclerosis we also evaluated the sex effect in our statistical model and found for H3K27Me3 a significant effect ($p = 0.006$; data not shown).

To estimate the specificity of the H3K27Me3 antibody, IHC with antibodies directed against H3K9Me3, H3K4Me3 and H3Ac was also performed in a number of cases. Both H3K9Me3 and H3K27Me3 are associated with transcriptional repression whereas H3K4Me3 and H3Ac are associated with transcriptional activation.

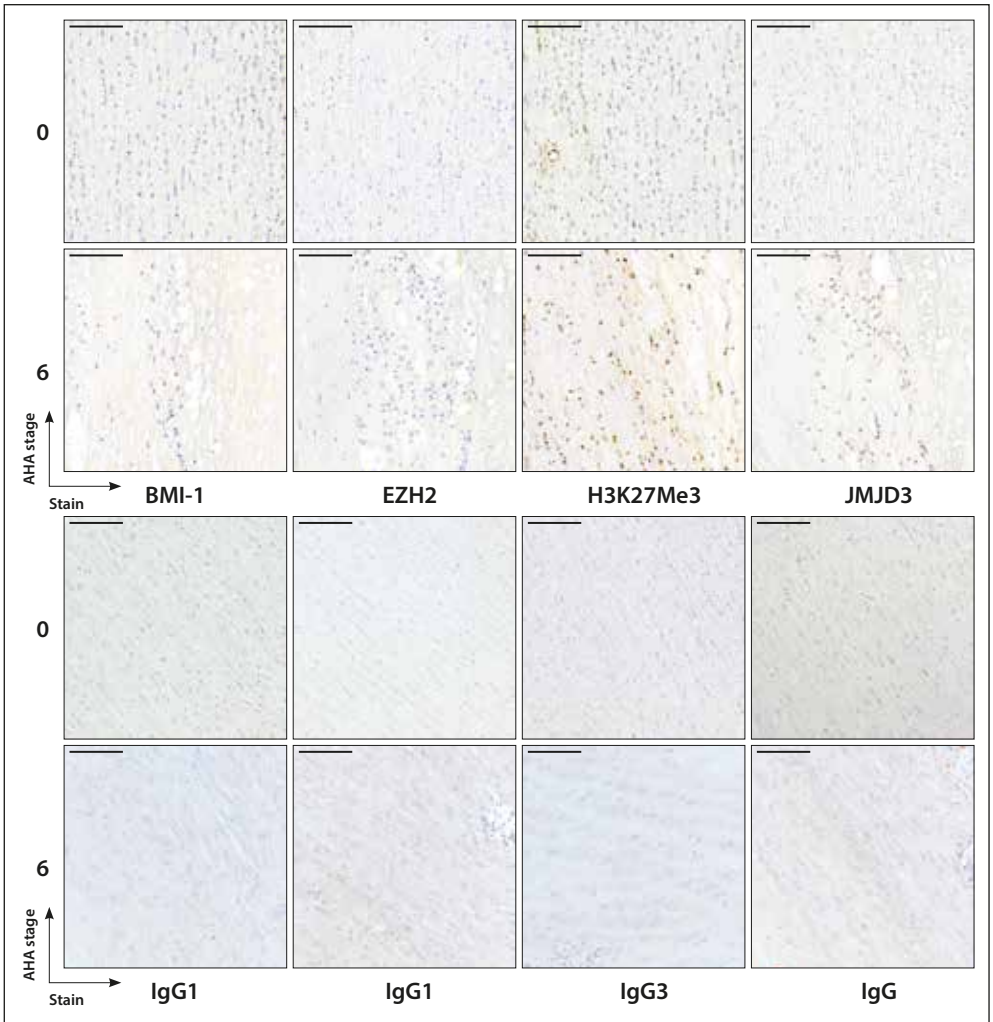

Figure 2–1. Representative staining for BMI1, EZH2, H3K27Me3, JMJD3 (upper panel) and their respective isotype controls (lower panel) staining in a normal vessel (stage 0) and an advanced plaque vessel (stage 6). Scale bars indicate 100 µm.

Shown in figure 2–5 (upper panel), is the staining pattern for H3K4Me3, H3Ac, H3K9Me3 and H3K27Me3 in vasculature-associated lymphoid tissue (VALT). Since VALT has a higher cell density, staining patterns are more easily discriminated. The staining patterns for H3K4Me3 and H3Ac marks are noticeably distinct from the H3K27Me3 and H3K9Me3 marks. Staining patterns for H3K9Me3 and H3K27Me3 show more similarities, but still yield a distinctively different pattern.

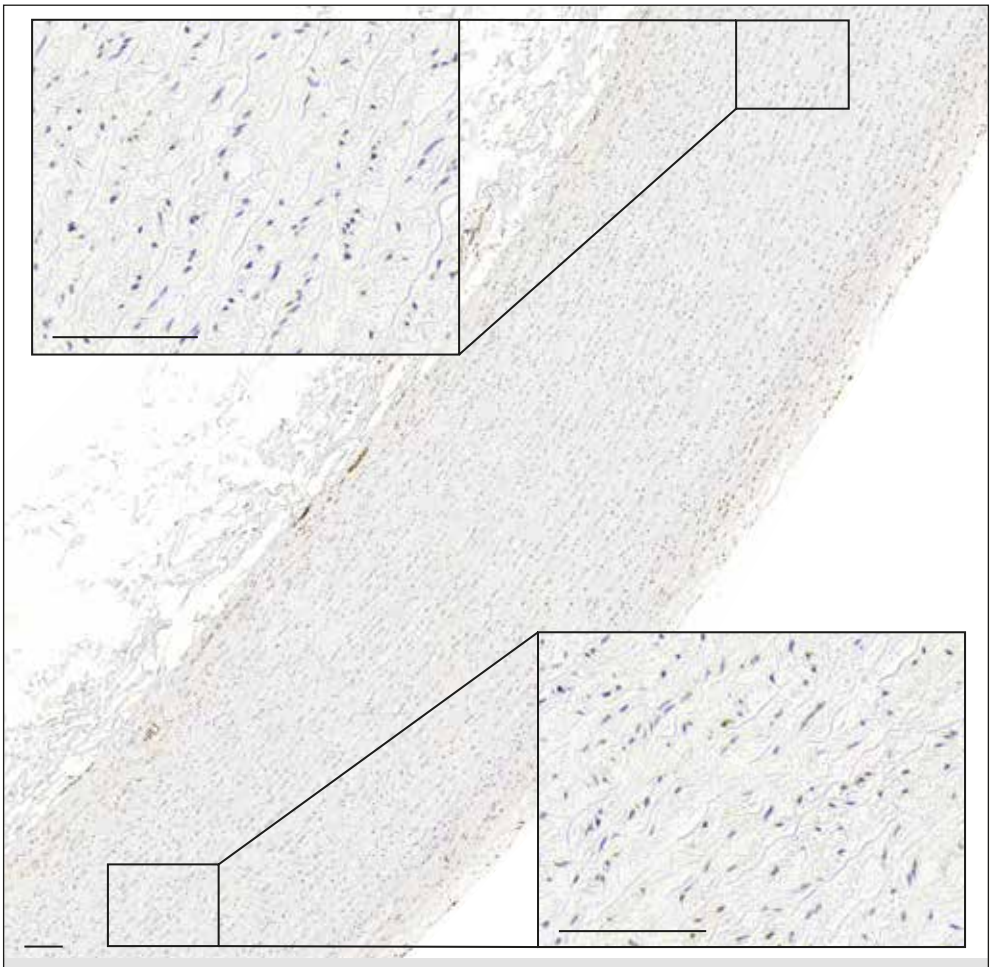

Figure 2–2. Representative slide showing nuclear H3K27Me3 staining in a normal vessel (stage 0) of a 16–year-old female. Staining is non-homogeneous throughout the vessel wall. Differential staining-patterns can clearly be observed between the *tunica intima*, media and adventitia, as well as focal staining within the *tunica media*. Scale bars indicate 100 µm.

Besides assessing VALT, the *tunica media* of vessels was also assessed to estimate the specificity of the H3K27Me3 antibody used in IHC. The staining for H3K4Me3, H3Ac, H3K27Me3 and H3K9Me3 yield patterns distinctive from each other (Figure 2–5, lower panel), although it is harder to visually discern the staining pattern in the tunica media compared to in VALT. Together, these distinct staining patterns reflect the specificity of the H3K27Me3 antibody for detecting the H3K27Me3 histone mark.

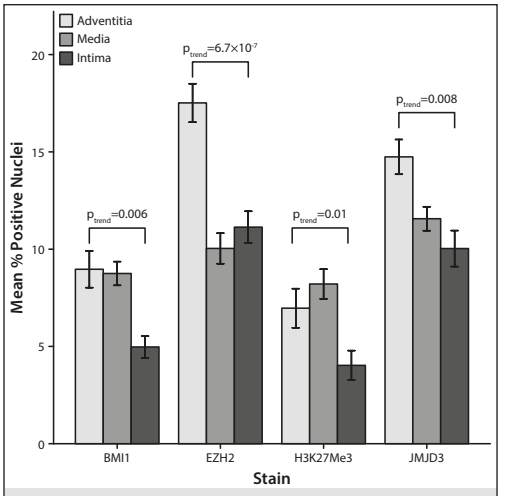

Figure 2–3. Percentage of positive nuclei found in *tunica intima*, *media* or *adventitia*. A significant increase of positively stained cells can be found in the *tunica adventitia* when compared with the intima, regardless of the used antibody. Error bars indicate ±SEM.

To further define the vessel wall components driving this change in global H3K27Me3 abundance, we investigated the distribution of this mark across the various vessel layers and plaque stage. As revealed in figure 2–6 all three layers showed lower levels in the number of nuclei displaying the H3K27Me3 mark. However, the reduction in the global levels of H3K27Me3 was more pronounced in the *tunica media* of vessels with late stage atherosclerotic plaques. The numbers of nuclei that reacted with the anti-EZH2, anti-JMJD3 and anti-BMI1 antibodies in the various vessel wall components remained similar in vessels with early and vessels with late stage atherosclerotic plaques (data not shown).

Correlation between H3K27Me3 levels and BMI1, EZH2 and JMJD3 levels

Given the functions of EZH2, JMJD3 and BMI1, a correlation between H3K27 Me3 levels and EZH2, JMJD3 and BMI1 levels can be expected. Correlations between the various staining levels were tested using Pearson's correlation. We found a weak correlation between levels of H3K27Me3 and BMI1 ($p = 0.014$; $r = 0.494$; Figure 2–7), but no correlation between levels of H3K27Me3 and JMJD3 or EZH2 (Figure 2–7).

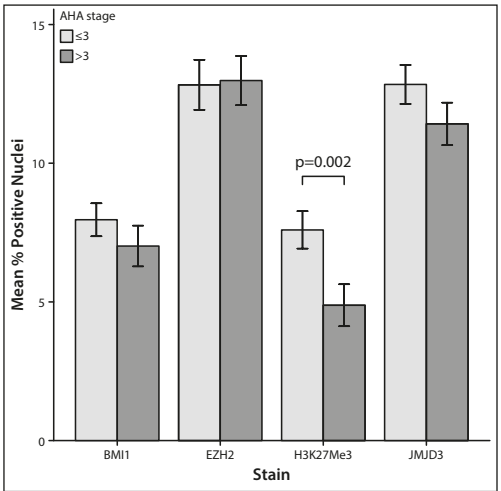

Figure 2–4. Quantitative analysis of staining patterns. Shown is the percentage of nuclei staining positive for proteins involved in H3K27Me3 methylation (i.e. BMI1, EZH2, JMJD3) and the H3K27Me3 mark itself, in early and late stage atherosclerotic plaques. A significant reduction of the H3K27Me3 mark was observed in more advanced lesions. Error bars indicate ±SEM.

Discussion

Currently it is widely appreciated that epigenetic processes contribute to disease pathogenesis including atherosclerosis. This is illustrated by recent research, which showed global alterations in DNA methylation in patients with CVD.[19–21] Some studies have also shown effects of small molecule inhibitors that interfere in the activities of histone modifying enzymes on disease parameters such as plasma cholesterol levels (see Wierda *et al.*[2] and references therein). In a previous study from our institute using the ApoE mouse model, an association between histone methylation and diet-induced hypercholesterolemia in vSMCs of ApoE+/– offspring from ApoE-deficient mothers was revealed.[15] In particular a significant decrease in vSMCs for global H3K27Me3 levels was noticeable following a high cholesterol diet postnatal in these ApoE+/– offspring.[15] A similar effect of this diet was also noted on global H3K27Me3 levels when offspring from wild-type mothers and ApoE-deficient mothers were compared.[15] To date, nothing is known with respect to alterations in global histone methylation patterns in human atherosclerotic processes. Therefore, in the current study, we have evaluated the association of global levels of H3K27Me3 with varying grades of atherosclerotic lesions. The results of this study revealed a significant decrease in the number of nuclei that stained positive for the H3K27Me3 repressive mark in vessels with late atherosclerotic lesions in comparison to vessels with early lesions. Particularly this difference was most pronounced in the *tunica media,* which comprises mostly vSMCs. Similar to the observations made in the ApoE-mouse model, high levels of cholesterol may contribute to the observed reduction in H3K27Me3 levels in the vessel wall of patients with advanced atherosclerotic plaques.

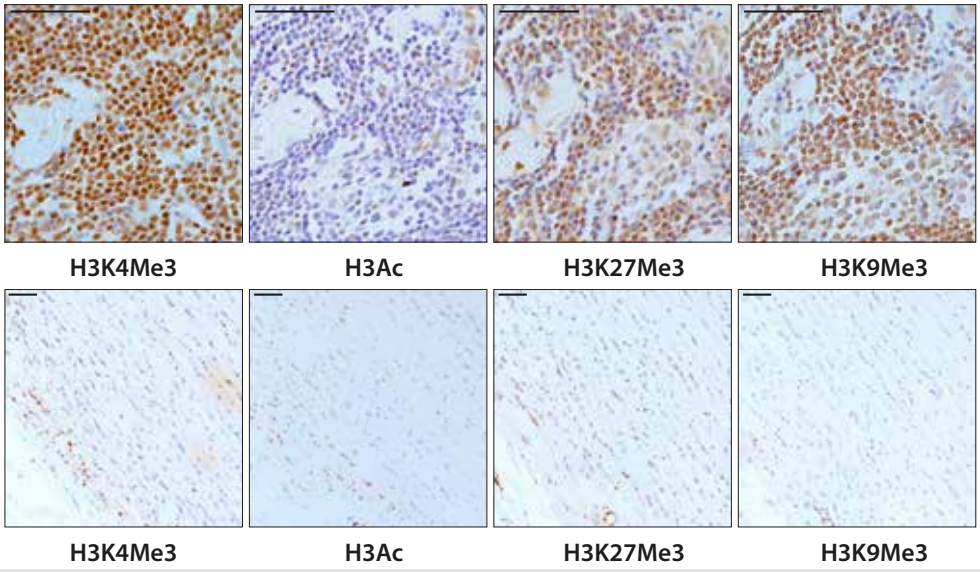

Figure 2–5. Specificity of the H3K27Me3 antibody was estimated by IHC staining with antibodies detecting other posttranslational modifications in histone H3 in serial sections of vasculature-associated lymphoid tissue (VALT) and of the tunica media. Shown in this figure are the staining patterns for H3K4Me3, H3Ac, H3K9Me3 and H3K27Me3. (Upper panel): Staining in VALT of a vessel with a ruptured plaque (stage 6) of a 57–year-old male. Since VALT has a higher cell density, staining patterns are more easily discriminated. The H3K4Me3 and H3Ac marks (associated with transcriptional activation) are notably distinct from the H3K27Me3 mark (associated with transcriptional repression). Staining patterns for H3K9Me3 and H3K27Me3, both marks being associated with transcriptional repression, show a higher degree of similarity. (Lower Panel): Staining pattern in the *tunica media* in a normal vessel (stage 0) of a 16–year-old female; vessel is identical to the vessel shown in figure 2–2. The H3K4Me3, H3K9Me3 and H3Ac marks all show a visually distinct pattern from the H3K27Me3 mark. Scale bars indicate 50μm.

We also studied the association of EZH2, BMI1 and JMJD3 in these atherosclerotic processes. No significant differences were observed in the number of nuclei that reacted with the immune reagents against EZH2, BMI1 and JMJD3 between vessels with early (including normal vessels) or with late atherosclerotic plaques. Therefore, no direct correlations could be made between levels of H3K27Me3 and levels of EZH2 (in the context of the PRC2 complex, the writer of the H3K27Me3 mark), of BMI1 (in the context of the PRC1 complex, the reader of the H3K27Me3 mark) or with JMJD3 (the eraser of the H3K27Me3 mark). The percentage of immunopositive H3K27Me3 and BMI1 nuclei however does show a significant, albeit weak correlation. This provides an indication that the observed change in H3K27Me3 results in a PRC-controlled cellular response.

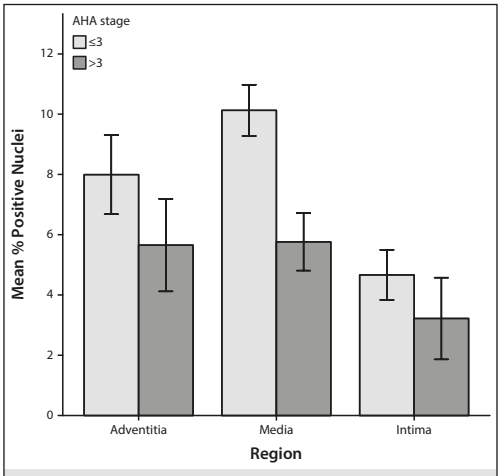

Figure 2–6. Location of H3K27Me3 within the vessel wall for early and late stage atherosclerotic plaques. A reduction of H3K27Me3 levels can be observed in all layers of the vessel wall. The most pronounced reduction of H3K27Me3 can be observed in the *tunica media*. Error bars indicate ±SEM.

The change in global histone modification levels without a change in the associated writer or eraser, observed in this study, has been noted before as well.[22] In a different study it was observed that, although EZH2 levels were significantly increased between patients and controls, there was no difference in global H3K27 methylation levels in PBMCs of patients with psoriasis vulgaris.[23] It must furthermore be realized that IHC does not address the functional activities of the proteins investigated or the catalytic capacity of the active complexes.

Of interest is the notion that regardless of the antibody used in the immunohistochemical staining, there is significantly more staining in the *tunica adventitia*. This is most likely a reflection of the cell types commonly found in the adventitia, which differ from those in the *tunica media* and *tunica intima*. A most likely explanation is that (activated) immune cells present in the *tunica adventitia* contribute to this skewing.

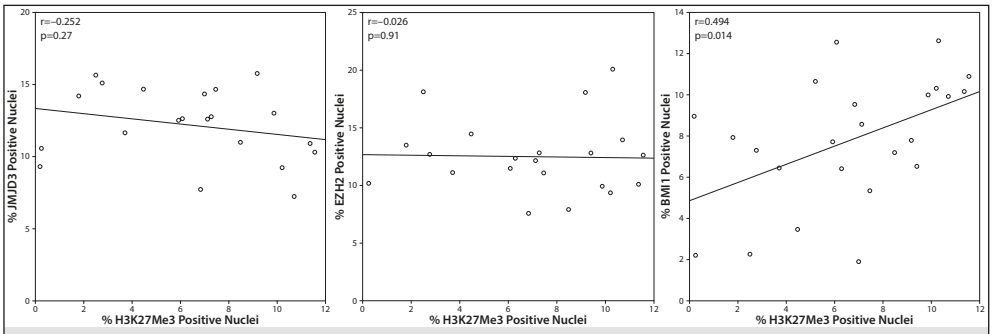

Figure 2–7. Correlations between H3K27Me3 levels and BMI1, EZH2 and JMJD3 levels. Correlations were tested, using Pearson's correlation, between the percentage of immunopositive H3K27Me3 nuclei and JMJD3, EZH2 or BMI1 immunopositive nuclei. No correlation was found between the percentage of H3K27Me3 immunopositive nuclei and JMJD3 or EZH2 immunopositive nuclei. A significant, albeit weak, correlation was found between the percentage of H3K27Me3 immunopositive nuclei and BMI1 immunopositive nuclei.

Interestingly, in vessels with advanced plaque stages, the observed decrease in H3K27Me3 positively stained cells occurs mostly in the *tunica media*. Given the role of the H3K27Me3 modification in chromatin condensation and gene silencing, the reduction in global H3K27Me3 levels in the *tunica media* infers that chromatin accessibility is increased, which could affect also the rate of transcription of genes involved in cell proliferation. This may reflect the proliferation of vSMCs commonly described in plaque formation. Whether this decrease in global H3K27Me3 levels proceeds or follows vSMC proliferation remains to be established.

In previous *in vitro* studies, a relation was found between cell activation and JMJD3 expression in macrophages.[11,12] In these studies cultured cells were subjected to LPS stimulation for several hours. Peak JMJD3 expression occurred after 2 hours whereafter JMJD3 levels diminished, showing that this is a temporary event. Both inflammation and macrophages form a central hub in the pathology of atherosclerosis. However, neither early, nor advanced atherosclerotic plaques showed significant alteration in JMJD3 levels in the various vessel wall components. The use of cross sectional material in this present study makes it therefore very unlikely to encounter macrophages that have been activated in the same time frame as in these previous *in vitro* studies.[11,12] Secondly, although macrophages are one of the major constituents of atherosclerotic plaques, they are present in relatively small numbers when the entire cross-section is taken into account, as in this study. Even if the effect observed by De Santa *et al.*[11,12] is present in human atherosclerotic plaques, it will probably not be reflected in the type of data we show here. Finally, the effect seen in the study by De Santa *et al.* may have been a LPS-specific effect, whereas LPS is not commonly associated with atherosclerosis.

Limitations of the current study

IHC results are notoriously hard to quantify, as staining intensity is not always correlated with protein concentration.[24] Furthermore DAB staining does not follow Lambert Beers Law complicating quantification. Also, DAB and heamatoxillin are hard to spectrally unmix by image processing.[25] In the data presented here, the heamatoxillin staining is often overpowered by strong DAB intensity. Using immunofluorescence the limitation of spectral unmixing could be overcome, but care must be taken in correlating intensity to protein expression with regards to quantitative analysis. The results presented here would therefore need to be confirmed by more quantitative methods, such as western blotting or ELISA. By using such methods distribution of protein expression across tissue however will be lost.

Trimethylation of H3K27 plays a definitive role in random X-chromosome inactivation26 and lineage determination.[27,28] It could therefore be expected that all, or at least a large number of cells of female-derived vessels stain positive for H3K27Me3 or for the commonly expressed modifying proteins EZH2, JMJD3 and BMI1. However, the seemingly low level of immunopositive nuclei that we found both in normal and in atherosclerotic vessels is observed quite frequently also in other studies. In several studies aimed to evaluate global levels of specific histone acetylation and methylation modifications it has been shown, both in humans and in mice, that these histone modifications, including H3K27Me3, are not detected in the nucleus of every cell by IHC.[15,29–31] This seemingly lack of the presence of a specific histone acetylation or methylation modification in the nucleus could be the due to the detection limitations of IHC. However, given the fact that this type of staining pattern has previously been observed in IHC,[15,29–31] it would be very unlikely that in the current study this relates to atherosclerosis pathology.

Conclusion

Our findings reveal the dynamics in the numbers of nuclei that display the H3K27Me3 mark during disease progression. The reduction in the number of nuclei that display the H3K27Me3 could reflect a phenotype switching of vSMCs. Due to sensitivity limitations of the current study, these results need to be confirmed by more quantitative methods.

Because epigenetic processes are involved in the transcriptional regulation of many, if not all genes, it remains to be elucidated which specific genes whose products contribute to atherosclerosis formation are actively controlled by H3K27Me3 in these different vSMCs (see Wierda *et al.*[2] and references therein). With many environmental risk factors contributing the atherosclerosis development, epigenetic phenomena may hold the key to understanding the onset and progression of this disease. Furthermore, these enzymes may also prove to be effective targets for clinical management of the disease, given the wide availability of Small Molecule Inhibitors that interfere in the activities of the enzymes that modify histones by acetylation or by methylation.

Acknowledgements

This research was financially supported in part by the Translation of Excellence in Regenerative Medicine (TeRM) Smart Mix Program of the Netherlands Ministry of

Economic Affairs and the Netherlands Ministry of Education, Culture and Science, the Macropa Foundation and the Department of Immunohematology and Blood Transfusion. We thank R.A. van Dijk for his technical assistance and Prof. Dr. W.E. Fibbe for his support.

Conflicts of interest

The authors declare that there are no conflicts of interest.

References

1. O'Toole, T.E., Conklin, D.J. & Bhatnagar, A. Environmental risk factors for heart disease. *Rev Environ Health (2008)*; **23**, 167–202. doi:10.1515/REVEH.2008.23.3.167
2. Wierda, R.J., Geutskens, S.B., Jukema, J.W., Quax, P.H.A. & van den Elsen, P.J. Epigenetics in atherosclerosis and inflammation. *J Cell Mol Med (2010)*; **14**, 1225–40. doi:10.1111/j.1582-4934.2010.01022.x
3. Jenuwein, T. & Allis, C.D. Translating the histone code. *Science (2001)*; **293**, 1074–80. doi:10.1126/science.1063127
4. Morey, L. & Helin, K. Polycomb group protein-mediated repression of transcription. *Trends Biochem Sci (2010)*; **35**, 323–32. doi:10.1016/j.tibs.2010.02.009
5. Schuettengruber, B., Chourrout, D., Vervoort, M., Leblanc, B. & Cavalli, G. Genome regulation by polycomb and trithorax proteins. *Cell (2007)*; **128**, 735–45. doi:10.1016/j.cell.2007.02.009
6. Cao, R. & Zhang, Y. The functions of E(Z)/EZH2-mediated methylation of lysine 27 in histone H3. *Curr Opin Genet Dev (2004)*; **14**, 155–64. doi:10.1016/j.gde.2004.02.001
7. Visser, H.P., Gunster, M.J., Kluin-Nelemans, H.C. et al. The Polycomb group protein EZH2 is upregulated in proliferating, cultured human mantle cell lymphoma. *Br J Haematol (2001)*; **112**, 950–8. doi:10.1046/j.1365-2141.2001.02641.x
8. Schuringa, J.J. & Vellenga, E. Role of the polycomb group gene BMI1 in normal and leukemic hematopoietic stem and progenitor cells. *Curr Opin Hematol (2010)*; **17**, 294–9. doi:10.1097/MOH.0b013e328338c439
9. Sasaki, M., Ikeda, H., Sato, Y. & Nakanuma, Y. Decreased expression of Bmi1 is closely associated with cellular senescence in small bile ducts in primary biliary cirrhosis. *Am J Pathol (2006)*; **169**, 831–45. doi:10.2353/ajpath.2006.051237
10. Lan, F., Bayliss, P.E., Rinn, J.L. et al. A histone H3 lysine 27 demethylase regulates animal posterior development. *Nature (2007)*; **449**, 689–94. doi:10.1038/nature06192
11. De Santa, F., Totaro, M.G., Prosperini, E. et al. The histone H3 lysine-27 demethylase Jmjd3 links inflammation to inhibition of polycomb-mediated gene silencing. *Cell (2007)*; **130**, 1083–94. doi:10.1016/j.cell.2007.08.019
12. De Santa, F., Narang, V., Yap, Z.H. et al. Jmjd3 contributes to the control of gene expression in LPS-activated macrophages. *EMBO J (2009)*; **28**, 3341–52. doi:10.1038/emboj.2009.271
13. Gehani, S.S., Agrawal-Singh, S., Dietrich, N. et al. Polycomb group protein displacement and gene activation through MSK-dependent H3K27me3S28 phosphorylation. *Mol Cell (2010)*; **39**, 886–900. doi:10.1016/j.molcel.2010.08.020
14. Leung, C., Lingbeek, M., Shakhova, O. et al. Bmi1 is essential for cerebellar development and is overexpressed in human medulloblastomas. *Nature (2004)*; **428**, 337–41. doi:10.1038/nature02385
15. Alkemade, F.E., van Vliet, P., Henneman, P. et al. Prenatal exposure to apoE deficiency and postnatal hypercholesterolemia are associated with altered cell-specific lysine methyltransferase and histone methylation patterns in the vasculature. *Am J Pathol (2010)*; **176**, 542–8. doi:10.2353/ajpath.2010.090031
16. van Dijk, R.A., Virmani, R., von der Thusen, J.H., Schaapherder, A.F. & Lindeman, J.H.N. The natural history of aortic atherosclerosis: a systematic histopathological evaluation of the peri-renal region. *Atherosclerosis (2010)*; **210**, 100–6. doi:10.1016/j.atherosclerosis.2009.11.016
17. Stary, H.C., Chandler, A.B., Dinsmore, R.E. et al. A definition of advanced types of atherosclerotic lesions and a histological classification of atherosclerosis. A report from the Committee on Vascular Lesions of the Council on Arteriosclerosis, American Heart Association. *Circulation (1995)*; **92**, 1355–74. doi:10.1161/01.CIR.92.5.1355

18. Ruifrok, A.C. & Johnston, D.A. Quantification of histochemical staining by color deconvolution. *Anal Quant Cytol Histol (2001)*; **23**, 291–9. doi: not available

19. Stenvinkel, P., Karimi, M., Johansson, S. et al. Impact of inflammation on epigenetic DNA methylation – a novel risk factor for cardiovascular disease? *J Intern Med (2007)*; **261**, 488–99. doi:10.1111/j.1365-2796.2007.01777.x

20. Sharma, P., Kumar, J., Garg, G. et al. Detection of altered global DNA methylation in coronary artery disease patients. *DNA Cell Biol (2008)*; **27**, 357–65. doi:10.1089/dna.2007.0694

21. Lund, G. & Zaina, S. Atherosclerosis: an epigenetic balancing act that goes wrong. *Curr Atheroscler Rep (2011)*; **13**, 208–14. doi:10.1007/s11883-011-0174-3

22. Miao, F., Smith, D.D., Zhang, L. et al. Lymphocytes from patients with type 1 diabetes display a distinct profile of chromatin histone H3 lysine 9 dimethylation: an epigenetic study in diabetes. *Diabetes (2008)*; **57**, 3189–98. doi:10.2337/db08-0645

23. Zhang, P., Su, Y., Zhao, M., Huang, W. & Lu, Q. Abnormal histone modifications in PBMCs from patients with psoriasis vulgaris. *Eur J Dermatol (2011)*; **21**, 552–7. doi:10.1684/ejd.2011.1383

24. Watanabe, J., Asaka, Y. & Kanamura, S. Relationship between immunostaining intensity and antigen content in sections. *J Histochem Cytochem (1996)*; **44**, 1451–8. doi:10.1177/44.12.8985137

25. Taylor, C.R. & Levenson, R.M. Quantification of immunohistochemistry--issues concerning methods, utility and semiquantitative assessment II. *Histopathology (2006)*; **49**, 411–24. doi:10.1111/j.1365-2559.2006.02513.x

26. Plath, K., Fang, J., Mlynarczyk-Evans, S.K. et al. Role of histone H3 lysine 27 methylation in X inactivation. *Science (2003)*; **300**, 131–5. doi:10.1126/science.1084274

27. Morgan, H.D., Santos, F., Green, K., Dean, W. & Reik, W. Epigenetic reprogramming in mammals. *Hum Mol Genet (2005)*; **14 Spec No 1**, R47–58. doi:10.1093/hmg/ddi114

28. Ng, R.K., Dean, W., Dawson, C. et al. Epigenetic restriction of embryonic cell lineage fate by methylation of Elf5. *Nat Cell Biol (2008)*; **10**, 1280–90. doi:10.1038/ncb1786

29. Nakazawa, T., Kondo, T., Ma, D. et al. Global histone modification of histone H3 in colorectal cancer and its precursor lesions. *Hum Pathol (2012);* **43**, 834–42. doi:10.1016/j.humpath.2011.07.009

30. Cai, M.Y., Hou, J.H., Rao, H.L. et al. High expression of H3K27me3 in human hepatocellular carcinomas correlates closely with vascular invasion and predicts worse prognosis in patients. *Mol Med (2011)*; **17**, 12–20. doi:10.2119/molmed.2010.00103

31. Tzao, C., Tung, H.J., Jin, J.S. et al. Prognostic significance of global histone modifications in resected squamous cell carcinoma of the esophagus. *Mod Pathol (2009)*; **22**, 252–60. doi:10.1038/modpathol.2008.172